

PACS numbers: 42.62.Be; 42.66.Ct
DOI: 10.1070/QE2002v032n10ABEH002314

Adaptive system for eye-fundus imaging

A.V. Larichev, P.V. Ivanov, N.G. Iroshnikov, V.I. Shmalhauzen, L.J. Otten

***Abstract*. A compact adaptive system capable of imaging a human-eye retina with a spatial resolution as high as 6 μm and a field of view of 15° is developed. It is shown that a modal bimorph corrector with nonlocalised response functions provides the efficient suppression of dynamic aberrations of a human eye. The residual root-mean-square error in correction of aberrations of a real eye with nonparalysed accommodation lies in the range of 0.1 – 0.15 μm.**

Keywords: *eye aberrations, wavefront sensor, modal wavefront corrector.*

1. Introduction

Optical methods have now found a widespread use in diagnosis of pathologies of a human retina. However, most attempts to obtain the retinal image with a spatial resolution limited by the diffraction from the eye pupil remain unsuccessful. It is known that a human eye, which has no apparent pathology of refraction, can be considered as approximately diffraction-limited only for a small (2 – 3 mm) diameter of the pupil. In case of a larger diameter, the spatial resolution is limited by random aberrations. Due to these aberrations, introduced by the cornea, crystalline lens and vitreous body [1, 2], the diameter of the entrance pupil of devices for studying the eye fundus (fundus cameras) should be limited to 2 mm.

Currently, the adaptive-optics-based techniques, allowing the compensation of random eye aberrations and, consequently, the extension of the entrance-pupil diameter of the device to 5 – 7 mm, are being intensely developed. In 1994, Liang proposed for the first time to use the Shack – Hartmann wavefront sensor for determining eye aberrations [3].

A.V. Larichev International Teaching and Research Laser Center, M.V. Lomonosov Moscow State University, Vorob'evy Gory, 119992 Moscow, Russia; Institute on Laser and Information Technologies, Russian Academy of Sciences, Svyatozerskaya ul. 1, 140700 Shatura, Moscow oblast, Russia; e-mail: larichev@iname.ru;
P.V. Ivanov, N.G. Iroshnikov, V.I. Shmalhauzen Department of Physics, M.V. Lomonosov Moscow State University, Vorob'evy Gory, 119992 Moscow, Russia; e-mail: ivpavel@iname.ru;
L.J. Otten Kesttrel Corporation, 3815, Osuna N.E., Albuquerque, New Mexico, 87109-4430 USA

Received 20 June 2002
Kvantovaya Elektronika **32** (10) 902 – 908 (2002)
Translated by Yu.M. Mikhailova

For this purpose, the laser radiation was directed into the eye and focused by eye elements on the retina, thus forming a reference source. The scattered radiation, emerging from the eye, was directed to the wavefront sensor. The first successful attempt to compensate for static eye aberrations was made in 1997 by the authors of [4]. They used the adaptive optical system including the Shack – Hartmann sensor and monolithic 37-electrode deformable mirror. The correction of phase distortions made it possible to discern the mosaic formed by photoreceptors of the retina with the characteristic size of 6 μm.

The first models of a Shack – Hartmann sensor did not allow eye aberrations to be measured at a high speed. This limitation arose from the fact that the speckle field, formed in the process of laser beam scattering by the retina, significantly lowered the quality of the detected signal. To suppress speckles, the time integration over the range from 200 to 400 ms was applied.

In 2001, the dynamic sensors, measuring phase distortions of the eye in real time, were fabricated. The experiments [5, 6] revealed that eye aberrations fluctuate in time. To suppress speckle structure in dynamic sensors, the authors of [6] scanned the position of the reference source on the retina, while the authors of [5] used a source with a low spatial coherence. This very year, the possibility to compensate for the dynamic phase distortions by means of a membrane mirror [7] and a bimorph corrector [8] was demonstrated. However, in [8] the retinal image was not registered.

Hofer et al. [9] experimentally compared the quality of eye aberration correction in cases of static and dynamic control of a 37-electrode monolithic mirror. The Shack – Hartmann wavefront sensor used in experiments measured aberrations with the 30-Hz rate. The analysis showed that the dynamic compensation increases the Strehl ratio by a factor of three and contrast of observable photoreceptors by 33 % compared to the static compensation. The field of view of the system was 1° under these conditions. However, for clinical applications, devices with the field of view of 10 – 30° are of the greatest interest. Therefore, the significant increase in the visual angle of adaptive systems is required to image the retina.

Generally, the field of view of the adaptive system, when examining the human eye, is limited by two factors: the imperfection of the image-forming optics and anisoplanar effects in the optical system of the eye.

Analytical estimates, analogous to those of paper [10], showed that in most cases for the pupil diameter of 5 mm, sufficient to observe even the smallest eye-fundus details

with respect to diffraction limitations, the isoplanar field of view reaches 7.5–15° (depending on the amplitude of eye aberrations and their distribution between the crystalline lens and the cornea). Thus, with an optical imaging system free of intrinsic aberrations in the angular field of about 15°, one can expect that the adaptive system will be able to compensate for distortions within the entire isoplanar area.

It is known that the amplitude of eye aberrations decays sharply with the increase of their order number [11]. Low-order aberrations such as the defocusing, astigmatism, coma and spherical aberration have the maximum amplitude. Monolithic and membrane mirrors allow one to correct only for aberrations with relatively low amplitudes. In this connection, in experiments [4, 7, 9] the defocusing and astigmatism were compensated before the feedback closure by means of the additional lens optics. In paper [12], the possibility to use a 69-segment liquid-crystal corrector for this purpose was examined. However, the authors failed to achieve a desirable effect and came to a conclusion that the dynamic range and the number of segments of a corrector should be significantly increased to compensate for real eye aberrations. Thus, the issue of optimal choice of a wavefront corrector for compensation of eye aberrations remains open.

There is another type of wavefront correctors yet not been used in adaptive compensation of human eye aberrations – modal deformable mirrors [13, 14]. Using a small number of control channels, such correctors allow a high-precision modelling of low-order aberrations with relatively high amplitudes. This property of such correctors corresponds to the statistical properties of phase distortions of the eye.

The response functions of modal correctors are non-localised: when applying the control voltage at any chosen electrode, the entire mirror changes its form. This fact substantially impedes the control of such a mirror.

In this paper, we introduce an adaptive system for eye-fundus imaging with a field of view of 15°, which consists of the dynamic Shack–Hartmann wavefront sensor and a modal bimorph corrector.

2. Experimental

The scheme of the experimental setup is shown in Fig. 1. The optical system is based on a KFG-2 fundus camera, series-produced by the Zagorsk Optics and Mechanics Plant joint-stock company (AO ZOMZ). Optical elements belonging to this device are circumscribed on the scheme by the dotted line. The standard fundus camera is supplemented with an adaptive unit, allowing the compensation of eye aberrations and retina imaging by means of a high-

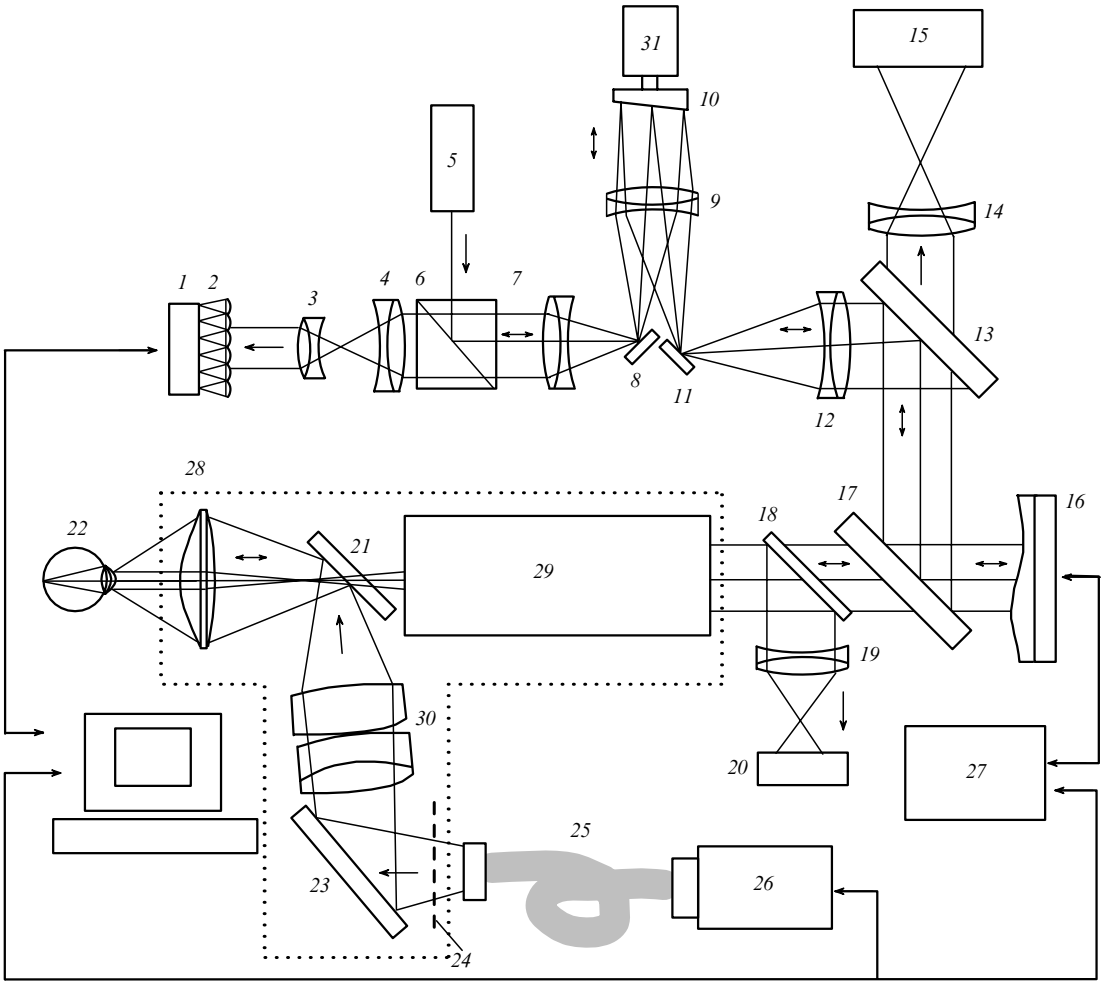

Figure 1. Scheme of the experimental setup: (*1, 20*) CCD cameras; (*2*) lens raster; (*3, 4, 7, 9, 12, 14, 19*) lenses; (*5*) laser; (*6*) beamsplitter cube; (*13, 17, 18*) beamsplitters; (*8, 10, 11, 21, 23*) mirrors; (*15*) digital camera; (*16*) adaptive mirror; (*22*) eye; (*24*) annular diaphragm; (*25*) fibreglass bundle; (*26*) illuminator unit; (*27*) adaptive mirror control unit; (*28, 30*) objectives; (*29*) fundus camera objectives; (*31*) electric motor.

resolution digital camera. The adaptive unit has $23 \times 23 \times$ 30-cm dimensions.

The series model of KFG-2 underwent a number of modifications. To improve the diffraction-limited resolution of the system to 200 lines per mm (the resolution value is determined at the half-maximum of the modulation transfer function), the diameter of the entrance pupil of this device was extended from 2 mm to 4.8 mm. The illuminating halogen lamp and pulsed xenon lamp with the corresponding collecting optics, as well as power supplies of these lamps, were removed. The observation binocular, employed for pointing of the fundus camera at the human eye, was replaced by an IR guidance system including the lens (*19*) and the IR CCD camera (*20*).

To illuminate the fundus of the examined eye in both the guidance and the digital photo-registration regimes, the illuminator (*26*) was fabricated. A 300-W cw xenon lamp with a small arc gap was used as a light source. Emission of the lamp was collimated by the built-in parabolic reflector and was incident on a movable mirror mounted on the axis of an electromagnetic drive (these elements are not shown in the scheme). In a stand-by mode, the mirror was removed from the light beam. When a control pule was applied, the mirror turned, thus directing the beam to a focusing lens and further to the end of the fibreglass bundle (*25*), which coupled radiation into the optical unit of the fundus camera. Therefore, the duration of the light flash directed into the eye depended on the length of the control pulse applied to the mirror. Different narrowband filters could be mounted between the deflecting mirror and the focusing lens, thus making it possible to photograph the eye fundus in different spectral ranges. To filter the IR emission, a spectral beamsplitter transmitting only visible light and reflecting near infrared was mounted in the illuminator. This beamsplitter also directed the IR emission of the halogen lamp, used for the guidance of the fundus camera to the patient's eye, to the optical path.

The illuminating radiation, propagating in the fibreglass bundle, passed through the annular diaphragm (*24*). The objective (*30*) imaged this diaphragm on the deflecting annular mirror (*21*), which was used to separate the illuminating beams, propagating in forward and backward directions, from each other. The main objective (*28*) of the camera imaged the annular light source on the eye cornea (*22*), with the central part of the cornea remaining unlit. The entrance pupil of the device was located entirely inside the unlit area. This provided an additional selection of corneal flares. Thus, spurious reflections did not appear in the area of the entrance pupil, and did not cause the artefacts in the retinal image. This illumination system also provided the uniform lighting of the eye fundus. A more detailed description of operation principles of such ophthalmologic devices can be found in papers [15, 16].

The radiation reflected by the retina emerges from the eye as a quasi-parallel beam. The eye-pupil image was constructed in the plane of the annular mirror (*21*) by the main objective (*28*) of the camera. The beam diameter corresponded to the central aperture of the annular mirror. Next, radiation propagated through the objective (*29*), fixed to the device, providing the transverse displacement and allowing the compensation of the eye ametropia within the range from -20 to $+20$ D.

After passing through the optical elements of the fundus camera, the light was incident on the spectral beamsplitter (*18*). A part of emission, corresponding to the IR emission (800 – 1000 nm) of the halogen lamp, was deflected by the beamsplitter to the guidance system. The lens (*19*) formed the retinal image in the plane of the IR video camera (*20*). The image registered by the video camera was displayed by the computer monitor and was used for the focusing of the fundus camera to the selected area of the retina.

Light, having passed through beamsplitters (*18*) and (*17*), was incident on the adaptive mirror (*16*). We used a modal bimorph corrector, which was similar to that described in paper [8]. Eighteen electrodes of the mirror made it possible to compensate for aberrations of up to the fifth order inclusive. The surface of the mirror was conjugate to the plane of the eye pupil and to the entrance pupil of the fundus camera.

The beam reflected by the deformable mirror was incident on the beamsplitter (*13*), transmitting the visible 440 – 670-nm light and reflecting the 680 – 800-nm radiation. The transmitted radiation passed through the lens (*14*), which formed the eye-fundus image on the matrix of the TsFK3020 digital video camera. One pixel of this camera corresponded to the retina region of size 2.7-μm. The photosensitive matrix had the resolution of 2000×3000 pixels. The signal of the matrix was digitised by means of the 14-bit ADC. For typical levels of the retina illumination, the camera provided the signal-to-noise ratio of 68 dB. The data transmission rate to the computer, provided by the digital interface, was one frame per second.

The configuration of the wavefront sensor is in many respects similar to the device described in paper [6]. The 780-nm radiation of the IR diode laser was used to form a reference light source on the retina. IR radiation of this range has the high coefficient of reflection from the eye fundus (10 % – 12 %) [17], and is more comfort for a human eye than visible light. Moreover, having chosen such a wavelength of the reference source, we separated the channel of the forming of the visible-light image of the retina from the aberration-measuring channel using the coherent IR radiation, by selecting the spectral characteristics of optical elements of the system.

Preliminarily, the laser beam (*5*) passed through the diaphragm (not shown in Fig. 1) of diameter 0.8 mm. The reduction of the beam diameter provided the conditions of single-pass measurements [18]. The power of radiation incident on the eye was 50 μW, which was significantly lower than the maximum permissible power [19, 20]. Then, the beam reflected from the inner face of the polarisation cube (*6*), propagateed through lenses (*7, 9*), and (*12*), reflected from the adaptive mirror (*16*), and was directed into the optical channel of the fundus camera. After passing through the objectives (*29*) and (*28*), the laser radiation was focused by the eye elements onto the retina, forming the reference source. The radiation scattered by the retina was brought back to the system, and was directed to the Shack – Hartmann wavefront sensor after the reflection from the adaptive mirror (*16*). The lens raster of the sensor (*2*) was placed in the plane, which was optically conjugated to the plane of the eye pupil. Each lens (subaperture) of the raster had a 0.25-mm diameter and a 7.8-mm focal length. For the pupil diameter equal to 4.8 mm, radiation emerging from the eye illuminated about 120 subapertures of the raster. The wavefront under study was divided by the lenses of the sensor, thus, forming an array of spots (Hartmannogram) in the focal plane. Each spot of the Hartmannogram was an

image of the reference source on the retina. The Hartmannogram was recorded by a CCD camera (*1*), located in the focal plane of the lens raster, and then was stored in the computer memory with the rate of 30 frames per second and the resolution of 640×480 pixels.

The wavefront was reconstructed from measured local wavefront slopes by the method of least squares [21] as an expansion in 36 Zernike polynomials [22] and in response functions of the adaptive mirror. The time of processing of a Hartmannogram was 8 ms. Thus, the maximum speed of aberration measurement was limited by the video camera parameters (30-Hz frame rate).

The speckle field, appearing upon scattering of the coherent laser radiation by the retina, lowers the quality of the Shack – Hartmann sensor signal and increases the error of the aberration measurement [6]. To suppress speckles in our system, we used the method of scanning of the reference-source position on the retina. For this purpose, the mirror (*6*) was attached to the electric-motor axis at a small angle equal to 0.5°. The rotation of the mirror caused the displacement of the reference source on the retina, resulting in a change in the speckle structure. For the electric-motor rotation speed of 50 rps, the characteristic time of a change in the speckle structure (0.2 ms) was much shorter than the integration time of the CCD camera (*1*) (30 ms), and, therefore, speckles were efficiently suppressed.

Because the laser radiation was twice (in a forward and backward passage) reflected from the scanner mirror, the displacement of the reference source on the retina did not cause any displacement of the Hartmannogram spots. This is explained by the fact that the eye mainly works as a retro reflector, i. e., radiation scattered by the retina emerges from the eye at an angle equal to the angle of radiation incidence. Because the surface of the scanner mirror was optically conjugated to the entrance pupil of the system and the lens raster of the sensor, wavefront slopes caused by this mirror were compensated during the backward passage.

The response functions of the modal bimorph corrector are not completely orthogonal. This fact complicates the sensor controlling procedure. To orthogonalise the response functions, the electrodes were combined into 11 groups. The control voltage was simultaneously applied with different weights to all the electrodes of a group. The weights were experimentally determined from the condition that the response functions should be maximally close to Zernike functions. In most cases, the residual error of compensation of real-eye aberrations was less than 0.1 – 0.15 μm. When the correction error reached this value, a computer automatically produced a synchronising signal for the illuminator, and the eye fundus was photographed.

Note that the scanning technique, applied in phase distortion measurements, has an important feature, which does not concern speckle suppression. The human eye, as the most of optical systems, is not isoplanar [23]. This means that the measured phase distortions depend on the angular position of the reference source. In this case, it is impossible to determine aberrations in the entire field of view of the system by using a single reference source [24]. Therefore, the adaptive compensation improves the image quality only within the isoplanatism region. In some cases, it is preferable to correct for average aberrations in a large field of view and to improve the image quality within the large area, than to achieve a high resolution within the small area.

The scanning technique, as distinct from other methods, gives an opportunity to determine average aberrations by using only one reference source. Thus, while laser spot moves sufficiently fast, the phase distortions are being averaged over the scanning area. The size of this area can be varied by changing the mirror tilt angle. In this work, we are not interested in compensation of average aberrations. In our case, the reference source described on the retina circle of 150-μm diameter. At present, no experimental data are available on the degree of anisoplanatism of the real human eye. Nevertheless, we can assume, relying on theoretical estimates [10], that in our case the displacement of laser spot was significantly smaller than the radius of isoplanatism.

The human-eye retina reflects a small part of the incident light [17]. In the experiment, the power of infrared radiation emerging from the eye did not exceed 5 μW. Although all lenses were covered with antireflection coatings, the intensity of light reflected from lenses was comparable with that of useful signal. To suppress spurious reflections, the polarisation cube (*6*) was set in such a way as to transmit the depolarised radiation scattered by the retina and to reflect polarised radiation scattered from optical surfaces. A diaphragm (not shown in Fig. 1), which also partially suppressed defocused reflections, was placed in the focal plane between lenses (*3*) and (*4*).

3. Compensation of eye-model aberrations

We used in our experiments the model of an eye representing an objective with a focal length $f = 20$ mm and an eye-retina-imitating scatterer (a fibreglass washer with fibre diameter of 6 μm). The front facet of the washer had a concave spherical surface with the radius of curvature equal to the radius of the focal surface of the objective. This allowed us to achieve precise focusing on the entire surface of the washer.

A standard USAF mire, also known as a '3-barred mire', was fastened by optical adhesive to the flat rear facet of the washer. The laser beam passing through the objective was focused on the front face of the washer. Then, light propagated through the fibres, reflected from the mire, propagated in backward direction, and formed a reference source on the front facet of the washer. Phases of radiation emerging from different fibres were uncorrelated. The fibreglass washer was fixed to a micrometer positioning stage, which provided the longitudinal displacement with the positioning accuracy of 10 μm.

The performance of the adaptive system is demonstrated in Fig. 2. Here, the images of the central part of the mire are shown in cases of open and closed feedback loop. To introduce phase distortions, the eyeglass lens of poor quality was placed in the plane of the artificial eye pupil at an angle to optical axis of the system. No preliminary compensation of defocusing by means of an adjustable objective of the fundus camera was performed. The mire was illuminated in this experiment from the back (with respect to the pupil of the eye model) side. Despite strong initial aberrations (the wavefront root-mean-square deviation was 1.2 μm), the adaptive compensation made it possible to resolve the horizontal 6 – 6-group lines of the mire with the spatial frequency of 114 lines per mm.

Note that employing of the fibreglass washer in the eye model does not allow the resolution of 7-group elements, which have the spatial frequency greater than 128 lines per

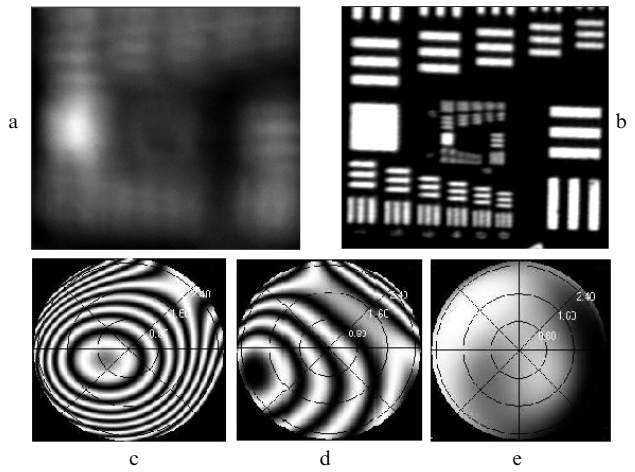

Figure 2. Images of the central part of the standard USAF mire for opened (a), and closed (b) feedback loop, and wavefront interferograms before compensation (c), before compensation, with eliminated defocusing (d), and after compensation (e).

mm. We cannot discern the details of the mire with sizes less than the fibre diameter. Indeed, the direct observation of the washer's surface under a microscope does not allow the resolution of 7-group elements as well. The interferograms of model eye-aberrations before the compensation, before the compensation with eliminated defocusing, and after the adaptive compensation are also shown in Fig. 2. In the latter case, the wavefront root-mean-square deviation was reduced to 0.07 μm.

4. Compensation of real-eye dynamic aberrations

The eye pupil was preliminary dilated by mydriatic eye drops (Phenylephrine Hydrochloride, 2.5 %) that do not paralyse accommodation. The dilation of the pupil allowed the use of its external side for the eye-fundus illumination, and the internal side – for the retina imaging. The patient's head was fixed by the face-holder of the fundus camera. All patients were instructed to look on a fixating needle (an infinitely far object) located inside the camera. The optical channel of the needle imaging and the channel of adaptive compensation were separated from each other; therefore, deformations of the adaptive mirror did not influence the eye accommodation.

The fundus camera was focused on the selected area of the retina with the help of the CCD camera (*20*). The eye aberrations were measured in real time, and the data were displayed on the monitor of the computer. As a preliminary to the feedback closure, the eye defocusing was compensated by means of the adjustable objective of the fundus camera. The Zernike coefficient corresponding to the defocusing was reduced to the minimum value under these conditions. This allowed us to use the entire dynamic range of the adaptive mirror. After feedback closure, the compensation of eye aberrations was performed. The eye fundus was photographed when the residual root-mean-square error of the compensation σ was reduced below 0.15 μm. However, in some cases, when aberration amplitudes (usually the astigmatism amplitude) exceeded the dynamic range of adaptive mirror deformations, we failed to achieve the satisfactory quality of suppression of phase distortions. Another, less common reason of poor-quality compensation was related to the low intensity level of the detected Hartmannogram, for example, due to the crystalline lens opacity.

During the xenon lamp flash, the laser and the illuminator lamp were switched off, and the control voltage applied to the mirror was 'frozen'. The light pulse duration was varied in the range from 30 to 100 ms. The eye fundus was photographed in different spectral ranges by filtering radiation of the xenon lamp emission at the output of the illuminator. The maximum intensity of the retinal illumination (in the absence of filters) was 0.08 J cm^{-2}. According to the American standard (ANSI), the maximum admissible illumination for the white light is 0.924 J cm^{-2} for the exposure time of 0.5 s [19].

Different spectral components of light are reflected from retinal layers lying at different depths. Because the laser wavelength was the same during the aberration measurement, the eye-fundus image was defocused when changing the spectral range of the light flash. To eliminate this effect (after the completion of the adaptive compensation), an additional voltage was applied to the main electrode of the deformable mirror just before the photographing. In this way, the defocusing, compensating for the displacement of the reflecting retinal layer, was introduced into the image-forming channel. By using different spectral bands, we obtained images of the retina layers of different depths.

An illustration of the adaptive compensation of eye aberrations is given in Fig. 3. Aberrations were detected for 10 s. The feedback loop was closed at the third second. No preliminary compensation of the defocusing (by means of the tunable objective of the fundus camera) was performed; therefore, the defocusing (curve *1*) was the predominant aberration (0.5 μm) before the feedback closure. The following-in-magnitude aberrations were the astigmatism (curve *2*) and coma (curve *3*). Aberrations of the order, higher than spherical, were low and are not shown in Fig. 3. One can see from the presented dependences that the process of the adaptive compensation lasted about 0.5 s. The root-mean-square phase deviation σ decreased under these conditions from 0.6 to 0.1 μm. The wavefront interferograms, written before and after the adaptive compensation, are shown in Fig. 3 as well. The interferogram of Fig. 3b

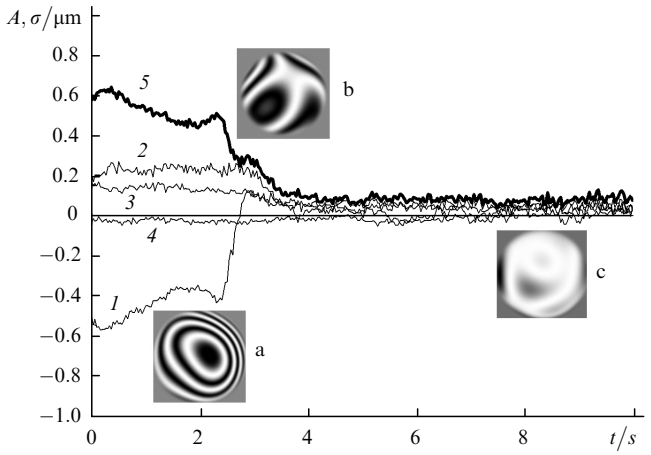

Figure 3. Time dependences of aberration amplitudes A: defocusing (*1*), total astigmatism (*2*), total coma (*3*), spherical aberration (*4*), and root-mean-square phase deviation σ (*5*). Aberration interferograms before compensation (a), before compensation, with eliminated defocusing (b), and after compensation (c).

corresponds to phase distortions before the feedback closure in the case of eliminated defocusing.

As is known, the eye defocusing fluctuates in time even for the fixed accommodation [25]. This fact impedes the manual eye-fundus focusing in standard fundus cameras. In this case, the focusing accuracy depends on subjective estimates, made during watching in viewfinder ocular, and on a personal experience of an observer. Therefore, an important feature of our system is that it is capable of compensating for the defocusing in an automatic mode.

Fig. 4 illustrates the improvement of the eye-fundus-image quality in the process of the adaptive compensation of eye aberrations. Here, two central parts of the retinal image, obtained in green light in cases of closed and opened feedback loop, are shown. For visual clarity, we do not show the complete image of the eye fundus, corresponding to the entire visual angle of our system (15°), and represent only a part of it, involving the optical disk (6-° visual angle).

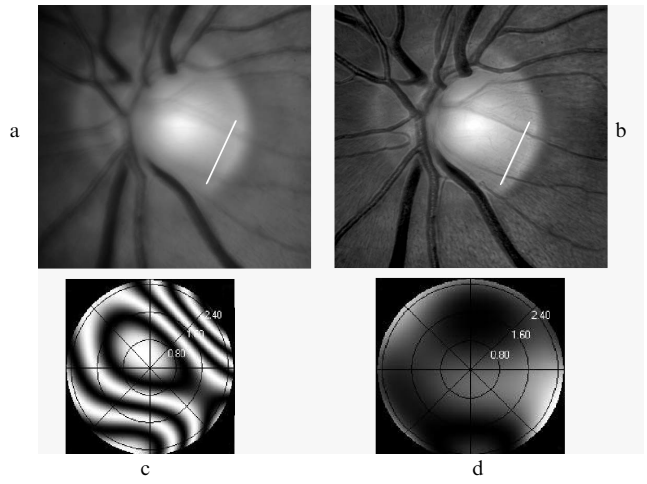

Figure 4. Images of optical disk of the eye retina for opened (a), and closed (b) feedback loop, and wavefront interferograms (c, d). White straight lines in Figs 4a, b denote cross sections, whose intensity distributions are shown in Fig. 5.

The refraction of the patient's eye was 2 D and the astigmatism was 1 D. As a preliminary to the feedback closure, the eye defocusing was compensated by means of the adjustable objective of the fundus camera. Fig. 4 also shows the interferograms of the wavefront before and after the correction of aberrations. After the feedback closure, the root-mean-square deviation of the wavefront decreased from 0.46 to 0.09 μm.

One can see from the given images that the compensation of eye aberrations substantially improved the image contrast and allowed the discerning of small details, being invisible on the first image with the compensation of eye defocusing. Thus, after the feedback closure, the nerve fibres lying on the retinal surface and directed to the centre of the optical disk can be discerned. Some separate nerve fibres, invisible in the blurred noncorrected image, are well distinct against bright background of the optical disk. The characteristic width of these fibres is about 3 μm and is comparable with the size of the camera pixel (2.7 μm). Due to the spatial discretisation of the image, we cannot reliably resolve all nerve fibres (the details with the characteristic size of less than 6 μm suffer aliasing). Nevertheless, some fibres are distinctly visible, which seemingly corresponds to the case when a fibre falls exactly on camera pixels.

For comparison, Fig. 5 shows the intensity distributions in the digital-image cross sections, cut through white lines drawn in Figs 4a and b. One can see that after the adaptive compensation, a pair of strong local minima, corresponding to a pair vessels lying on the optical disk, appeared in the intensity distribution $I(x)$. The intensity distribution of the corrected image has more of small (8-μm resolution) extrema as compared with the first image, which was obtained by compensating the eye defocusing only.

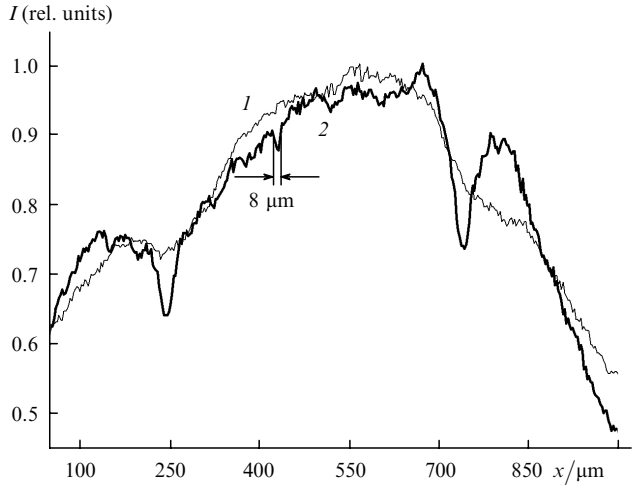

Figure 5. Intensity distributions $I(x)$ in the cross sections denoted in Figs 4a, b by white straight lines for opened (*1*), and closed (*2*) feedback loop.

5. Conclusions

We have developed an adaptive system for high-quality imagining of the eye fundus within a wide (15°) field of view.

We have shown that modal bimorph correctors provide the efficient compensation of the dynamic human-eye aberrations. The response functions of the adaptive mirror can be partially orthogonalised and the compensation quality can be improved by grouping of different electrodes of the bimorph corrector.

Unlike works [4, 9], where the accommodation-paralysing agents (Tropicamide) were used for the eye-pupil dilation, in our experiments the accommodation has not been paralysed. The authors of paper [26] showed that for frequencies up to 3 Hz the spectral density of time fluctuations of aberrations of the eye with nonparalysed accommodation is about 20 times higher in amplitude than the spectral density corresponding to the paralysed accommodation. Despite this fact, in our experiments, the residual root-mean-square error in the correction of real-eye phase distortions did not exceed 0.15 μm. This indicates that the system can efficiently suppress aberrations even in these, more difficult conditions.

The comparison between the results of correction obtained by means of the 18-electrode modal bimorph mirror and the results obtained with multielectrode correctors with the lumped response functions, allows us to conclude that the increase in the number of control channels

does not significantly affect the quality of the compensation of real-eye aberrations. In our opinion, this is explained by the fact that the amplitude of eye aberration sharply decreases with increasing their ordinal number, so that the high-order aberrations have no significant influence on the quality of the image.

The compactness of the developed adaptive system and the comparative ease of its control justify the optimistic forecasts of prospective clinical applications of adaptive systems.

Acknowledgements. The authors thank A.Yu. Resnyanski for his help in fabricating of measuring equipment and A. Goncharov for his help in developing the eye model. This work was supported by the NATO 'Science for Peace' programme (Project SfP 974292).

References

1. Artal P., Guirao A. *Opt. Lett.,* **23**, 1713 (1998).
2. Artal P., Berrio E., Guirao A., Piers P. *J. Opt. Soc. Am. A,* **19**, 137 (2002).
3. Liang J., Grimm B., Goelz S., Bille J.F. *J. Opt. Soc. Am. A,* **11**, 1949 (1994).
4. Liang J., Williams D.R., Miller D.T. *J. Opt. Soc. Am. A,* **14**, 2884 (1997).
5. Hofer H., Artal P., Singer B., Aragon J.L., Williams D.R. *J. Opt. Soc. Am. A,* **18**, 497 (2001).
6. Larichev A.V., Ivanov P.V., Iroshnikov N.G., Shmalhauzen V.I. *Kvantovaya Elektron.,* **31**, 1108 (2001) [*Quantum Electron.,* **31**, 1108 (2001)].
7. Fernndez E.J., Iglesias I., Artal P. *Opt. Lett.,* **26**, 746 (2001).
8. Larichev A., Irochnikov N., Ivanov P., Kudryashov A. *Proc. SPIE Int. Soc. Opt. Eng.,* **4251**, 102 (2001).
9. Hofer H., Chen L., Yoon G., Singer B., Yamauchi Y., Williams D.R. *Opt. Exp.,* **8**, 631 (2001).
10. Larichev A.V., Iaitskova N.A., Shmalhausen V.I. *Proc. II Intern. Workshop on Adaptive Optics for Industry and Medicine* (Durhum, Ingland, 1999) p. 272.
11. Guirao A., Porter J., Williams D.R., Cox I.G. *J. Opt. Soc. Am. A,* **19**, 1 (2002).
12. Vargas-Martin F., Prieto P., Artal P. *J. Opt. Soc. Am. A,* **15**, 2552 (1998).
13. Kudryashov A.V., Shmalhausen V.I. *Opt. Eng.,* **35**, 3064 (1996).
14. Dainty J.C., Koryabin A.V., Kudryashov A.V. *Appl. Opt. LP,* **37**, 4663 (1998).
15. Urmakher L.S., Aizenshtat L.I. *Oftal'mologicheskie pribory* (Ophthalmologic Instruments) (Moscow: Meditsina, 1988).
16. Tamarova R.M. *Opticheskie pribory dlya issledovaniya glaza* (Optical Devices for Examination of Eye) (Moscow: Meditsina, 1982).
17. Delori F.C., Pflibsen K.P. *Appl. Opt.,* **28**, 1061 (1989).
18. Diaz Santana Haro L., Dainty J.C. *Opt. Lett.,* **24**, 61 (1999).
19. *American National Standard for the Safe Use of Lasers, ANSI Z136.1* (Orlando, Fla., Laser Institute of America, 1993).
20. *Normy i pravila ustroistva i ekspluatatsii lazerov* (Norms and Regulations for Laser Arrangement and Operation) No. 5804-91 (Moscow, 1991).
21. Southwell W.H. *J. Opt. Soc. Am.,* **70**, 998 (1980).
22. Born M., Wolf E. *Principles of Optics* (Oxford: Pergamon Press, 1969; Moscow: Nauka, 1973).
23. Fried D. *J. Opt. Soc. Am. A,* **72**, 52 (1982).
24. Johnston D., Welsh B. *J. Opt. Soc. Am. A,* **11**, 394 (1994).
25. Charman W.N., Heron G. *Ophthalmic Physiol. Opt.,* **8**, 153 (1988).
26. Larichev A.V., Ivanov P.V., Irochnikov N.G., Kudryashov A.V. *Asian J. Phys.* (2002) (in press).